

promoting access to White Rose research papers



Universities of Leeds, Sheffield and York
<http://eprints.whiterose.ac.uk/>

This is an author produced version of a paper published in **Chemical Engineering Science**.

White Rose Research Online URL for this paper:
<http://eprints.whiterose.ac.uk/11205>

Published paper

Lozano-Parada, J.H., Zimmerman, W.B. (2010) *The role of kinetics in the design of plasma microreactors*, Chemical Engineering Science, 65 (17), pp. 4925-4930
<http://dx.doi.org/10.1016/j.ces.2010.03.056>

The role of kinetics in the design of plasma microreactors.

Jaime H. Lozano-Parada and William B. Zimmerman

Department of Chemical and Process Engineering;

University of Sheffield, Sheffield S1 3JD

Abstract

Miniaturisation of plasma reactors has the potential of low power operation. In general, the electric field strength in the gap between two electrodes increases proportionate to inverse of the gap width, so that it is possible to overcome the first ionization potential of the gas with a low voltage. However, plasmas are extinguished primarily by recombination at the walls. Wall collisions are enhanced by the greater surface area to volume ratio in microchannels, which also increases proportionate to the inverse of the gap width. If the plasma were well-mixed, then the plasma creation in the bulk would be balanced by extinction at the wall, providing no particular advantage with regard to low voltage / low power operation. However, the plasma is transferred from the bulk to the wall by ambipolar diffusion. If the operation of the plasma microreactor is essentially transient or batch, whether or not the reaction kinetics are comparable to or faster than ambipolar diffusion determines if there is a regime of operation in which a low voltage plasma discharge can generate a high yield of product. In this paper, this question is investigated with regards to the ozone formation reaction and a particular design of a microchannel plasma reactor, with parameters so chosen to arguably achieve low voltage operation. The focus of this paper is the simulation of the kinetics of the plasma reactions leading to ozone formation, which shows a time to completion that is comparable (10^{-2} s) or faster than the estimate of ambipolar diffusion time at these length scales. Preliminary results of a microchip reactor are consistent with this prediction.

§1 Introduction

The first microplasmas were created more than thirty years ago, built up ion by ion or atom by atom by trapping with electromagnetic fields and laser cooling, leading to the 1989 Nobel Prize of G. Demhelt and W. Paul. The subsequent supramolecular structures had both liquid-like configurations and gas-like dynamics. Microplasmas, however, are becoming fashionable again due to the potential for micro and nanotechnology to generate, manipulate and control them precisely at scales still much larger than the molecular scale, but much smaller than the conventional plasma reactor. The most remarkable features of plasmas are their reactivity and broad gamut of chemical transformations. Miniaturisation of plasmas, coupled with microfluidic and microelectronic technology, should bring potential benefits that enable scientific and engineering developments across a wide range of disciplines and application areas. Generation of plasmas in microchannels could control to great precision these chemical transformations. Integrated with the rapidly developing field of microfluidics, microchannel plasma generation could be an enabling technology across fundamental and applied science. For instance, generation of plasmas from hydrocarbon fuels can transform chemical energy to kinetic energy to electricity at very high ion temperatures. This leads to high efficiency, since conventional combustion is limited by heat generation. For onchip analysis and chemical-plant-on-a-chip, microplasma dynamics can lead to novel analytical devices and chemical microreactors.

Chemical plants of the future are expected to be highly specialized with tight control of atom efficiency in order to minimise environmental impact. One exciting technology which appears to have the potential to enable such development is the miniaturization of

plants onto “chips”, perhaps with a range of nanotechnological devices to manipulate molecules and achieve the required precise chemistry. These miniaturized chemical reactors will require a range of unit operations such as heat exchange, mixing and separation as well as transport of reactants and products. The flows involved will be through microchannels, driven either by pressure or by electroosmotic forces. Currently such miniaturization is being studied at the micrometre scale in reactor volumes going down to nano litres. Key to the effectiveness of such networked processing schemes is the provision of a wide gamut of tightly controlled reactor types that can generate a broad range of chemical transformations. The conventional promise of microchannel processing is both greater efficiency of resource usage, but also greater effectiveness in modes of delivery –just-in-time but also *in situ* (drug delivery, pathology lab-on-a-chip). Potentially, a plasma microreactor would add an important advantage: a wider range of product chemicals. Macro scale plasma reactors are extremely good at generating a broad array of chemical transformations due to their ability to overcome high activation energies of transitions states and due to the multiple excited species possible. Control, however, is difficult to achieve in conventional plasma reactors.

Miniaturization promises to enhance control through the use of microfluidics that can tailor fluid dynamics and through high but brief field gradients that can be electronically controlled and spatially precise. The combination should be able to customize selectivity for desired products or intermediate constituents in chemical processing for high added value molecules such as fine chemicals and pharmaceuticals. Miniaturisation of plasma reactors onto microchips also has the promise of producing the plasmas at *much lower voltages* than conventional scale reactors, and thus achieving *low power production*. We have implemented such a microchannel plasma reactor for the production of ozone using a capacitive coupling to a plasma source and matching impedance network to maximise the power coupling.

The mean kinetic energy of a plasma discharge is a unique function of the reduced field (E/N), with E the electric field strength and N the gas number density. Thus, in order to have similarity conditions with conventional discharges one needs to conserve this quantity. This implies that the electric field strength should be kept constant. The inventive step was the observation that decreasing the dimension between electrodes in a capacitive coupled discharge to the micron scale increases the electric field strength, thus, in order to preserve the regime of plasma kinetic energy the voltage required to sustain the discharge is lower, and with this, the power required to sustain the discharge is also decreased. This is a very important characteristic of microplasmas, the fact that microplasmas can be sustained at substantially lower power which translates into lower operation costs and higher portability. Given that the voltage is reduced at the expense of smaller gap distance, it is necessary to find a pressure regime which enables us to describe the discharge in terms of the continuum nature of the conservation equations. This means that in order to preserve the continuum character of the conservation equations the working pressure should be increased. Working at high pressures (1 bar in this case) comes as a natural working condition. This also implies a great advantage in economical terms since working at high pressure rather than vacuum avoids the use of

expensive vacuum equipment. Therefore, working at low voltages and high pressures is very convenient both in terms of capital and operative cost.

It has been hypothesized that a plasma discharge so created would be short-lived as plasma is extinguished by collisions with surfaces, and given the much higher surface area to volume ratio of a microchannel; the expected microchannel reactor would have any advantage of high electric field strength for the generation swamped by the proximity of the walls. Indeed, this is the rationale for conventional plasma reactors having a large distance from the electrodes to the walls for low recombination. Our plasma reactor achieved steady glow discharges in an oxygen feed at 170 volts AC, which is much lower than the conventional thousands of volts typically used. The purpose of this paper is to describe the rationale for how low voltage / low power operation can be achieved, with high yields, by trading off the effects of electric field strength and plasma extinction, by recognizing that the time scales for chemical kinetics and ambipolar diffusion of the electrons and ions control the reactivity of the plasma.

This paper is organized as follows. In section 2, the design is discussed and the experimental methods are presented. In section 3, a simulation showing the expected kinetics time scale for the completion of the ozone formation reaction is evaluated. In section 4, the implications of the microfluidic plasma reactor so designed are discussed, and conclusions are drawn.

§2 Design and experimental set up

Conventionally, the received wisdom is to produce ozone by using corona discharge generators in which a flux of air or oxygen is subjected to a high voltage discharge that dissociates the oxygen to produce ozone. It is well known that negative coronas produce ozone at efficiencies not higher than 16-20%. Our intention with this paper is to estimate the potential yield output and energy efficiency possible from miniaturization of the reactor. Our aim is to design a plasma microreactor which works at atmospheric pressure, and, due to the promise of tighter control by working at microscales, achieves greater yield. There are two key factors which influence the effectiveness of miniaturization. Downscaling could be beneficial from the energy usage perspective since, as said before, the reduced field (E/N) can be set at much lower voltages which reduces the power requirements of the power supply. However, downscaling has some drawbacks since quenching of plasma species at the walls becomes more rapid as the characteristic length is reduced and the pressure increased from conventional partial vacuum operation to atmospheric pressure. In this regime the electron number density tends to decrease significantly, so in order to keep the discharge self-sustained, the inter-electrode voltage must be increased, even though, as said above, this is much lower than in conventional coronas. This push for better efficiencies has provided the motivation for further seeking ways of reducing the electron losses at the walls.

It is well known in the plasma literature that the Paschen law gives the breakdown voltage for a gas V_b as a function of the pressure p and displacement distance d characteristic of the source, $V_b=f(pd)$. Since we expect to generate plasmas in scales less than 1mm, at atmospheric pressure, the argon and helium curves from [Moravej et al.,

2004] illustrate approximate voltages of 125V and 70V, both safely and easily achievable in laboratory conditions. That we have generated plasmas with characteristic scale of 800 μm in argon and oxygen already suggests feasibility in the scales of microchips (Lozano-Parada, 2007).

At atmospheric pressure the main diffusion mechanism is that of ambipolar diffusion. The values of ambipolar diffusivity for ions and neutral gas are approximately the same, typically around $10^{-5} \text{ m}^2/\text{s}$. For typical plasmas the electron temperature is around 3-5 eV and the ion temperature perhaps 0.05-0.1 eV. Then, the time for a plasma to diffuse a length of 1mm will take approximately $\tau_{\text{ambipolar}}=100 \text{ ms}$. Thus, to achieve high yield with such a plasma microreactor, the design trade-off which minimises the effect of wall recombination of the plasma are at submillimetre scales:

- (1) A reaction which has characteristic time scale τ_{reaction} for completion of the order of 10^{-1} s or faster, i.e. $\tau_{\text{reaction}} < \tau_{\text{ambipolar}}$
- (2) An “exposure time” that is of the same order as τ_{reaction} . The exposure time is the residence time of the plasma in the reactor if it is a continuous process or the time in which the electric field is turned on in a batch reactor. In an AC plasma source, this suggests that the period of oscillation $T_{\text{ac}} \sim \tau_{\text{reaction}}$.

Experimental Design

The schematic of the plasma microreactor is shown in Figure 1. The central element is the microreactor, which has the key feature of a microchannel with smallest dimension (the width) at the submillimeter scale. To respect the balance of ambipolar diffusion and ozone formation kinetics, the width was selected to be 800 μm . The microreactor has an inlet feed of pure oxygen gas at room temperature. The microreactor has the possibility of a second inlet feed-through which is closed off for this experiment. A fibre optics spectrometer (UV-VIS Ocean Optics) is mountable to capture the emission spectra. The plasma microreactor is actuated by a plasma source and impedance matching network that was tuned to achieve maximum power transfer and minimum voltage operation.

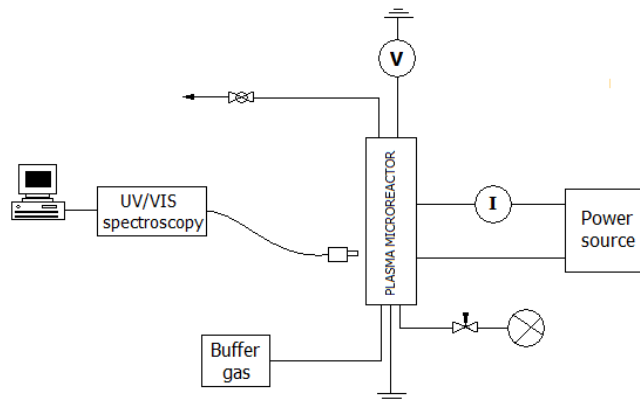


Figure 1: schematic of the layout of an ozone plasma microreactor and peripheral device connection.

Integral to the microreactor in Figure 1 is the implementation. Figure 2 shows the bespoke microchip which was microfabricated by electrodeposition of the copper electrodes on the sidewalls at the center of the microchannel over a length of 1cm. Masking precluded deposition elsewhere on the microchannel surfaces, particularly the microchannel floor. The fabrication was the modification of a standard chip by Micronit.

Figure 3 shows the upper and lower plates of the chipholder, including the mount points and connections for the gas inlets, outlets, and fibre optic cables.

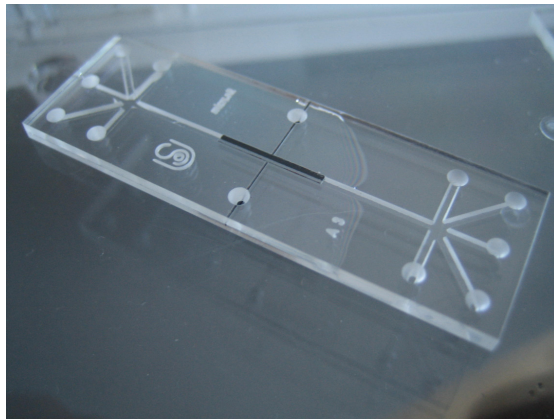


Figure 2: Microchip for the “control” experiment – stationary operation.

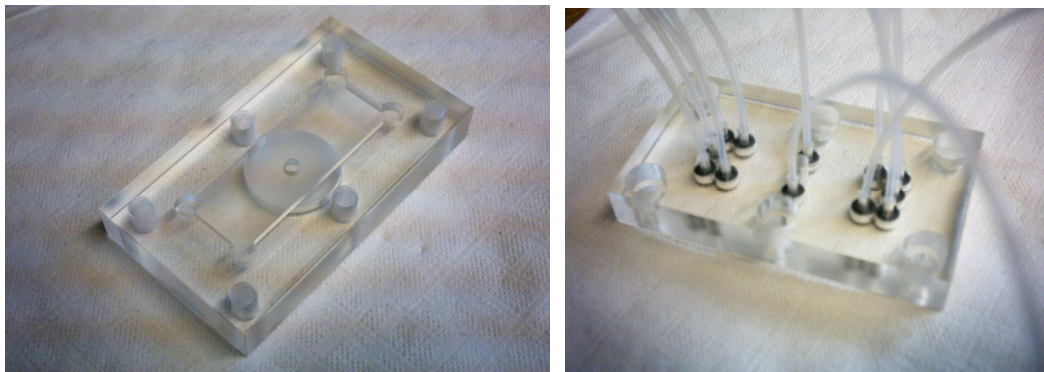


Figure 3: Chip holder (left) and with connectors to supply and outlet streams (right).

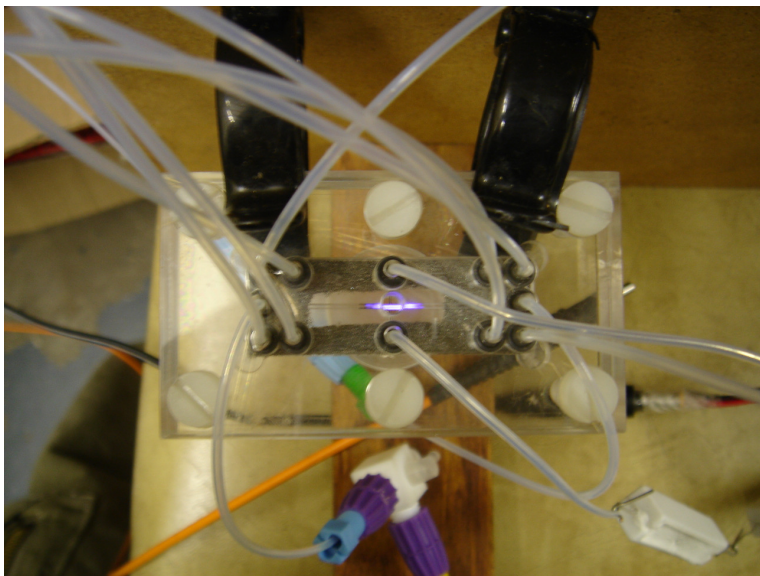


Figure 4: Glow discharge observed with AC plasma source at 170V.

Figure 4 demonstrates the observation of a glow discharge which is localized in between the electrode gap

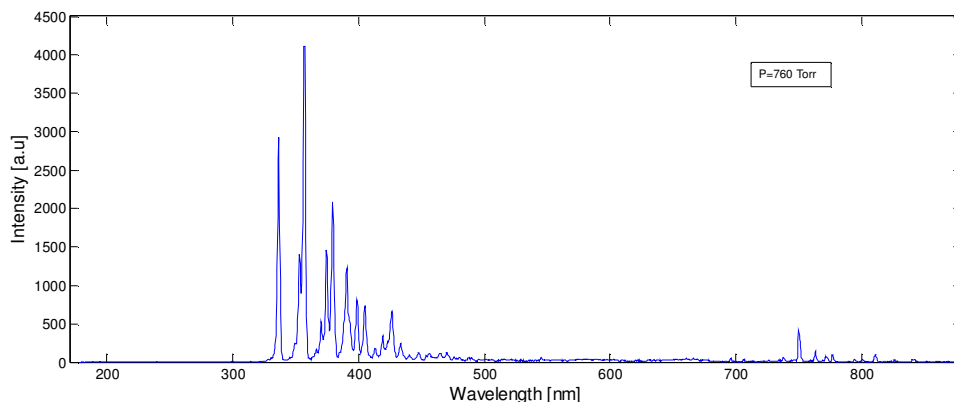


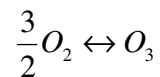
Figure 5: Emission spectrum of exit gas with clear O₃ signature between 400 nm and 500 nm. Analysis suggests 30% conversion at temperature 350K.

Emission spectra, such as Figure 5, of the discharge were obtained using an Ocean Optics[®] spectrometer. A fibre optic was attached to the optical port on the chip holder and the other end to the entrance slit of the spectrophotometer. The glass material with which the plasma chip was fabricated is a D263T glass from Schott[™]. It has a transmission window that allows us to obtain clear emission spectrums of ozone in the visible range. The chip holder was made of Perspex but care about its optical properties is not necessary to be taken since the optical emission from the discharge does not go through it.

According to Herzberg (1966), the UV-Vis spectrum of ozone consists of several bands: Hartley (220nm-300nm), Huggins (310nm–374nm) and Chappuis (550nm-610nm). Between 400nm and 500nm ozone has a very poor absorptivity so these bands show up in the spectrum of Figure 5 as strong emission bands which can be used according to Kylián *et al* (2003) to calculate the gas temperature, which was around 350 K. Also the ozone formation was calculated in this band which showed an ozone conversion of around 30% which constitutes a substantial improvement already compared to a conventional corona discharge.

§3 Ozone formation kinetics time scale

Ozone chemistry has an importance in several application areas. Unlike the diatomic oxygen, O₂, ozone is a powerful oxidizing agent. Ozone reacts with some gases, such as nitric oxide or NO, and with some surfaces, such as dust particles, leaves, and biological membranes. These reactions can damage living cells, such as those present in the linings of the human lungs. It is a photochemical atmospheric pollutant, formed only during daylight hours under appropriate conditions, but is destroyed throughout the day and night. Ozonolysis, the breakdown of complex organic chemicals under exposure to ozone, can be used for synthetic and analytic chemistry. Along with the depletion of the ozone layer in the atmosphere by chlorinated fluorocarbons, these uses make ozone a well studied molecule, with substantial kinetics data assembled for its formation and dissociation reactions. Lieberman and Lichtenberg (2005) have collated much of this kinetics information, and Lozano-Parada (2007) has an extensive review. Table 1 shows a subsystem of 21 reactions important in the overall reaction with stoichiometry:



This subsystem is most important in “cold” plasmas, i.e. low electron temperature and gas temperature near room temperature.

In this section, a chemical kinetics model for the conditions of the plasma microreactor demonstrated in section 2 is developed. The assumptions of such a model are that the reactor is well-mixed, such as a continuously stirred tank reactor. This assumption is consistent with the observation in section 2 that the ambipolar diffusion is not rapid enough for a transversely well mixed reactor during the first 10⁻² s. However, the kinetics model is developed here solely for the purpose of estimating the time scales of the ozone formation reaction.

Reaction index i	Reaction	Rate coefficient k_i (m^3/s , m^6/s)
1	$\text{e}+\text{O}_2 \Rightarrow \text{e}+2\text{O}$	$2\text{e}-15$
2	$\text{e}+\text{O}_3 \Rightarrow \text{e}+\text{O}+\text{O}_2$	$5\text{e}-15$
3	$\text{O}_3+\text{O} \Rightarrow 2\text{O}_2$	$1.8\text{e}-17*\exp(-2300/\text{T})$
4	$\text{O}_3+\text{O}_2 \Rightarrow \text{O}+2\text{O}_2$	$7.26\text{e}-16*\exp(-11400/\text{T})$
5	$\text{O}+2\text{O}_2 \Rightarrow \text{O}_3+\text{O}_2$	$6.4\text{e}-47*\exp(663/\text{T})$
6	$\text{e}+\text{O}_2 \Rightarrow \text{e}+\text{O}(1\text{D})$	$3.41\text{e}-16$
7	$\text{e}+\text{O}(1\text{D}) \Rightarrow \text{e}+2\text{O}$	$1.47\text{e}-16$
8	$\text{e}+\text{O}(1\text{D}) \Rightarrow \text{e}+\text{O}_2$	$1\text{e}-15$
9	$\text{O}+\text{O}(1\text{D}) \Rightarrow \text{O}+\text{O}_2$	$1.3\text{e}-22$
10	$\text{O}+\text{O}_3 \Rightarrow \text{O}(1\text{D})+\text{O}_2$	$1\text{e}-17*\exp(-2300/\text{T})$
11	$\text{O}_2+\text{O}(1\text{D}) \Rightarrow 2\text{O}_2$	$2.2\text{e}-24*(\text{T}/300)^(0.8)$
12	$\text{O}(1\text{D})+\text{O}_3 \Rightarrow \text{O}+2\text{O}_2$	$5.2\text{e}-17*\exp(-2840/\text{T})$
13	$\text{O}(1\text{D})+\text{O}_3 \Rightarrow \text{O}_2+\text{O}_3$	$4.55\text{e}-17*\exp(-2180/\text{T})$
14	$2\text{O}_3 \Rightarrow \text{O}+\text{O}_2+\text{O}_3$	$1.648\text{e}-15*\exp(-11400/\text{T})$
15	$3\text{O} \Rightarrow \text{O}+\text{O}_2$	$6.2\text{e}-44*\exp(-750/\text{T})$
16	$2\text{O}+\text{O}_2 \Rightarrow 2\text{O}_2$	$1.3\text{e}-44*(300/\text{T})*\exp(-170/\text{T})$
17	$2\text{O}+\text{O}_2 \Rightarrow \text{O}+\text{O}_3$	$2\text{e}-46*\exp(345/\text{T})$
18	$2\text{O}+\text{O}(1\text{D}) \Rightarrow \text{O}_2+\text{O}(1\text{D})$	$7.4\text{e}-45$
19	$2\text{O}+\text{O}(1\text{D}) \Rightarrow \text{O}+\text{O}_3$	$6\text{e}-46$
20	$\text{O}+2\text{O}_2 \Rightarrow \text{O}(1\text{D})+\text{O}_3$	$8.7\text{e}-49*\exp(-1690/\text{T})$
21	$\text{O}+\text{O}_2+\text{O}_3 \Rightarrow 2\text{O}_3$	$1.452\text{e}-46*\exp(663/\text{T})$

Table 1 Most important low temperature ozone pathway reactions and their rate coefficients for temperature dependence are known in the literature. Lieberman and Lichtenberg (2005) give tables of most of this kinetics information, and the rest is cited by Lozano Parada (2007). Temperatures T are measured in degrees Kelvin.

Kinetics model equations

The reactions in Table 1 are elementary, and can be assembled into a model for intrinsic chemical kinetics for the concentration of these five species. If the reactor is assumed kinetics dominated (well mixed) – when the reaction time is much shorter than the ambipolar diffusion time, then each of the elementary reactions in Table 1 contributes mass action law terms to the kinetics model with rate constants (including Arrhenius temperature dependence), with number densities defined as: n_e is the density of electrons; n_1 the density of O; n_2 the density of O_2 ; n_3 the density of O_3 and n_4 is the density of the excited state of oxygen $\text{O}(1\text{D})$

$$\begin{aligned}
\frac{dn_1}{dt} &= 2k_1n_en_2 + k_2n_en_3 - k_3n_3n_1 + k_4n_3n_2 - k_5n_1n_2^2 + 2k_7n_en_4 - k_{10}n_1n_3 \\
&+ k_{12}n_4n_3 + k_{14}n_3^2 - 2k_{15}n_1^3 - 2k_{16}n_1^2n_2 - k_{17}n_1^2n_2 - 2k_{18}n_1^2n_4 - k_{19}n_1^2n_4 \\
&- k_{20}n_1n_2^2 - k_{21}n_1n_2n_3 \\
\frac{dn_2}{dt} &= 0 \\
\frac{dn_3}{dt} &= -k_2n_en_3 - k_3n_3n_1 - k_4n_3n_2 + k_5n_1n_2^2 - k_{10}n_1n_3 - k_{12}n_4n_3 - k_{14}n_3^2 \\
&+ k_{17}n_1^2n_2 + k_{19}n_1^2n_4 + k_{20}n_1n_2^2 + k_{21}n_1n_2n_3 \\
\frac{dn_4}{dt} &= k_6n_en_2 - k_7n_en_4 - k_8n_en_4 - k_9n_1n_4 + k_{10}n_1n_3 - k_{11}n_2n_4 - k_{12}n_4n_3 \\
&- k_{13}n_4n_3 - k_{19}n_1^2 + k_{20}n_1n_2^2 \\
\frac{dn_e}{dt} &= 0
\end{aligned}$$

It is presumed that the concentration of diatomic oxygen is fixed in this hypothetical reactor at the ideal gas molar level and the electron density is set by the electric field strength.

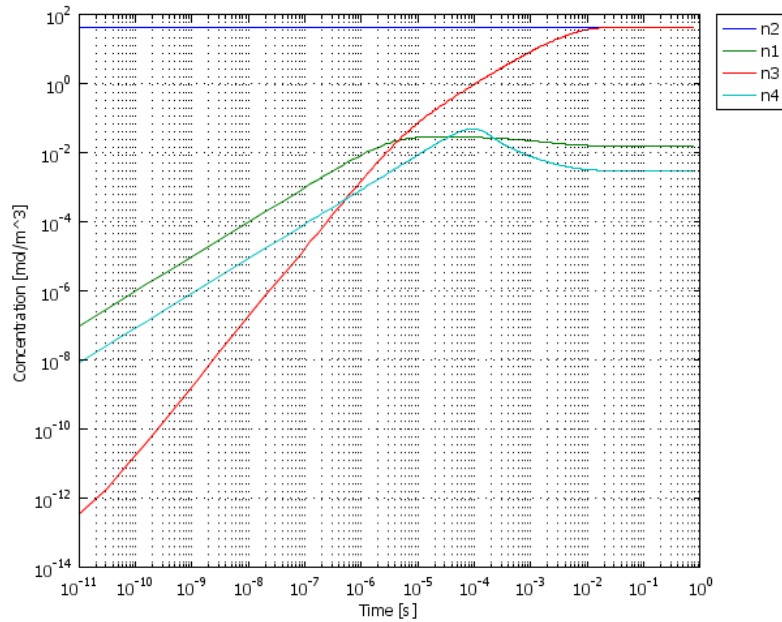


Figure 6: Species concentration evolution. n_e is the density of electrons; n_1 the density of O; n_2 the density of O₂; n_3 the density of O₃ and n_4 is the density of the excited state of oxygen O(1D)

The kinetics model was solved using the Reaction Engineering Laboratory of Comsol Multiphysics (see Zimmerman, 2006). The package has an automatic sensing of stiff systems and an adaptive time stepping algorithm with relative tolerance set to 10^{-6} .

Figure 6 shows the time evolution of the five species monitored in the kinetics model from pure O_2 initial conditions. This model uses only electrons and molecular oxygen as precursor species. The electrons are accelerated in the external electric field and collide with molecular oxygen to form ozone and other intermediate species. The initial condition for electron number density corresponds to the typical density of electrons in a gas at atmospheric pressure – n_e approx. 10^7 m^{-3} , and the initial condition for oxygen density is set according to an ideal gas law at room temperature and atmospheric pressure. The production rate of ozone is apparently exponentially rapid, with two different slopes in the log-log graph: roughly two and one, i.e. quadratic and linear growth. Given the small concentrations during the interval of the first slope, it is likely that only the later interval and slope are important in producing substantial yields of ozone. The kinetics model identifies two distinguished time scales for the ozone formation – the rate of formation in the linear regime and the time for completion of the reaction, i.e. the time for 99% of the equilibrium value. The later is approximately 10^{-2} s.

§4 Results and Discussion

Although the experimental configuration has been presented in section 2, it was for illustrative and motivational purposes only. Too little details are presented as the scope of the experimental system design, particularly the design and tuning of the plasma source and impedance matching network, are too complicated for anything other than a focussed presentation in a separate article. The range of conditions under which low voltage glow discharges can be achieved should also logically accompany that experimental design discussion, since the tuning of the plasma source is intimately related to the plasma dynamics. Furthermore, the variation of the experimental design, particularly the important role of dielectric barriers in reducing the impedance of the reactor / ionized gas should be fully investigated in such a sequel paper. The focus here is solely the time scale of the chemical kinetics given its importance to the low voltage design and operation envisaged here.

The simulations of §3 show that the time scale for the ozone generation is on the order of 0.01s, so that by the time (10-100 ms) that the plasma has diffused to the wall using the estimates of ambipolar diffusivity, the ozone generation reaction is complete. This result suggests that for any plasma reaction that is sufficiently fast, the microfluidic plasma reactor will achieve low power consumption at low voltages and atmospheric pressure. This is an approach to generate ozone on the small scale using approx 1/10 of the power of conventional ozone generation.

Conventional ozone generation involves the use of high voltage and high vacuum which both contribute to cost and safety risks. Our device uses low voltage – so the device can run off the mains and is safer – and does not require a vacuum. We believe that the ozone generation in this device is nearly three-fold higher than conventional techniques.

One of the many uses of ozone in industry is to purify and sterilise water. The conventional ozonation process uses twice the energy of chlorination and has a high capital cost. In the UK and other markets water is purified using chlorine for cost reasons even though ozonation leaves no noticeable taste. In countries such as France and Holland however, they prefer to use ozone on water taste grounds rather than cost.

By combining the microfluidic ozone generator with the novel aerator system (Zimmerman et al., 2008) it would be possible to create ozone rich micro-bubbles that could be used to purify the water. The generation of the ozone would be more efficient, and the delivery to the water by the microbubbles would be more efficient also. This could mean that conceivably only a small fraction of the existing ozonation rate would be needed to purify the water.

Conclusions

A microfluidic plasma reactor has been developed with a testbed application for the production of ozone.

The device has the important features for ozone generation:

1. Low power. Our estimates are a ten-fold reduction over conventional ozone generators for the same volume of ozone production.
2. High conversion. The selectivity is double that of conventional reactors - 30% rather than 15% single pass – making the process more efficient.
3. It does not need “special” operating conditions to work. It works at atmospheric pressure, at room temperature, and at low voltage – 170V – so it can be mains powered.
4. It does not need a pure oxygen source to produce ozone – it would work just as well with air.
5. It can be integrated with the recently patented microbubble dispersal system which achieves an order of magnitude higher dispersal rates than conventional bubble dispersal mechanisms. Such a plasma microreactor has been argued to trade-off in its design the effects of lower voltage / energy efficiency and the proximity of the walls increasing plasma extinction rates. Submillimeter reactor widths result in typical ambipolar diffusion times of (10-100 ms), so that only reactions with kinetics as fast or faster than this for completion time are relatively unaffected by the proximity of the walls. As the microchannel dimensions are further miniaturized, the extinction rates are expected to rise with the inverse power of the shortest dimension, while the electric field strength will rise with the same geometric scaling (with fixed voltage difference), indicating that the width which matches reaction completion time scale with ambipolar diffusion is the threshold for diminishing returns, and therefore should achieve optimum power requirement

Acknowledgements

The authors acknowledge support from the Basic Technology programme of the EPSRC (grant no. EP/D004748). We thank James Bradley, Bruce Ewan, and Christopher Whitehead for helpful discussions. We acknowledge technical support for microfabrication from Micronit.

References

- Agiral A., K. Seshan, L. Lefferts, J. G. E. Gardeniers, “Microplasma reactors with integrated carbon nanofibers and tungsten oxide nanowires electrodes” Proceedings of the Spring AIChE Meeting, 2008.
- Eijkel JCT, Stori H, Manz, “A dc microplasma on a chip employed as an optical emission detector for gas chromatography,” *Anal. Chem.* 72:2547—2552, 2000.
- Herzberg G., “Electronic spectra and electronic structure of polyatomic molecules”, Van Nostrand Reinhold, New York, 1966.
- Kylían O., Kaňka A. and Hrachová V., “Spectroscopic determination of oxygen DC glow-discharge temperature: Radial profile of gas temperature”, *Czechoslovak Journal of Physics*, 53(3), 2003.
- Lieberman M.A., A.J. Lichtenberg, Principles of Plasma Discharges and Materials Processing, 2nd ed., John Wiley and Sons, 2005.
- Lindner P. J. and R.S. Besser, “Reforming of JP-8 in microplasmas for compact SOFC power” Proceedings of the Spring AIChE Meeting, 2008.
- Lozano-Parada J. H., “Design, simulation and fabrication of a microchannel plasma reactor”, PhD thesis, University of Sheffield, 2007.
- Micronit Microfluidics BV: <http://www.micronit.com/>
- Moravej M. *et al.*, Physics of high pressure helium and argon radio frequency plasmas, *J. Appl. Phys.* 96(12):7011, 2004.
- Ocean Optics Spectrometer: <http://www.oceanoptics.com/Products/usb2000.asp>
- Zimmerman WBJ, Multiphysics Modelling with Finite Element Methods, World Scientific Series on Stability, Vibration and Control of Systems, Vol 18., Singapore, 2006.
- Zimmerman W.B, Tesař V, Butler SL, Bandulasena HCH, “Microbubble Generation”, *Recent Patents in Engineering*, 2:1-8, 2008.